1971

A study of the influence of gravity waves in a water-filled waveguide.

Ebert, Rolf Herbert.

A STUDY OF THE INFLUENCE OF GRAVITY WAVES IN A WATER-FILLED WAVEGUIDE

Rolf Herbert Ebert

NAVAL POSTGRADUATE SCHOOL
Monterey, California

THESIS

A STUDY OF THE INFLUENCE
OF
GRAVITY WAVES IN A WATER-FILLED WAVEGUIDE

by

Rolf Herbert Ebert

Thesis Advisor: A. B. Coppens

December 1971

A Study of the Influence of Gravity Waves in a Water-filled Waveguide

by

Rolf Herbert Ebert
Lieutenant Commander, Federal German Navy

Submitted in partial fulfillment of the requirements for the degree of

MASTER OF SCIENCE IN ENGINEERING ACOUSTICS

from the

NAVAL POSTGRADUATE SCHOOL
December 1971

ABSTRACT

A simple theory is developed which describes the fluctuation of a sound signal due to the influence of a standing gravity wave in a water-filled waveguide with idealized boundary conditions. The theory predicts a strong resonance of the fluctuation if the wave length of the surface wave is one-half of the acoustic wave length. The presence of this resonance is verified experimentally.

TABLE OF CONTENTS

LIST OF DRAWINGS

Figure

LIST OF SYMBOLS

x, y, z	rectangular coordinates
l_x, l_y, l_z	waveguide dimensions
k	acoustic wave number
k_i	acoustic propagation constant for the i^{th} direction
$\lambda = 2\pi/k$	acoustic wave length
ω	frequency of the acoustic signal in radians/sec
c	free-field acoustic phase speed
Φ	total acoustic velocity potential
Φ_1	acoustic velocity potential for the unperturbed case
ϵ	perturbation constant
t	time in sec
α	absorption coefficient of the cavity
β	absorption coefficient for the z-direction
γ	surface wave number
Ω	frequency of surface wave in radians/sec
a	surface wave amplitude
$\epsilon F(x,t)$	surface fluctuation
g	acceleration due to gravity

ACKNOWLEDGEMENT

The author wishes to acknowledge the support and encouragement provided him by Professor Alan B. Coppens. In addition the author wishes to thank technicians Robert Moeller, Thomas Maris, Milton Andrews, and Jack Brennan for their assistance.

I. INTRODUCTION

The influence of surface waves on guided mode propagation has been studied during the last 20 years. Particular attention was given to the amplitude fluctuation of the acoustic signal as a function of surface wave height and frequency spectra. J. A. Serimger [1] found a linear relationship between surface wave height and amplitude fluctuation of the acoustic signal. The linear coefficient increased with acoustic frequency. Furthermore he observed a fairly good match of the surface wave spectrum and the amplitude fluctuation spectrum. For larger wave heights the latter is broadened due to the presence of harmonics. R.A. D'Antonio and R. F. Hill [2] reported the same phenomena and give wide-band phase modulation credit for broading of the fluctuation spectrum, in particular for frequencies higher than those contained in the surface wave spectrum. A. B. Wood [3] conducted experiments in a tank and found the acoustic signal fluctuating at the frequency of the surface waves. With increasing wave height he observed a doubling of the fluctuation frequency. He believed that this was caused by an appreciable change of effective depth of the water above the transducer or by a peculiar reflection from the underside of the water waves.

R. J. Urick [4] placed a transducer at the bottom of a 60 foot deep water channel. Hydrophones were positioned 4300 feet away.

He observed two kinds of fluctuations of the acoustic signal: one was related to the frequency of the prevailing swell, and the other occurred at the tidal frequency. The relationship between amplitude fluctuation and the surface wave frequency was also found by C. S. Clay [5], and J. G. Clark and N. L. Weinberg [6]. P. J. Westervelt, H. Halpin, and A. O. Williams [7] extended Scrimger's work theoretically and experimentally. However, no explanation for the appearance of the harmonics could be found.

O. S. Tonakanov [8] investigated phase and amplitude of the signal as a function of wave height and of the distance between source and receiver. A recent experiment was done to detect a resonance effect of the amplitude fluctuation if the surface and acoustic wave lengths were matched [9, 10]. This resonance, predicted by a simple theory, could not be observed. A broad wind generated surface wave spectrum and other effects which could not be controlled might have masked the expected resonance.

The present work makes an attempt to prove the presence of this resonance by expanding the resonance theory and simplifying the experiment. A monochromatic surface wave is generated in a waveguide. The frequency of the acoustic signal propagating in the waveguide is changed and the amplitude of the acoustic fluctuations recorded as a function of frequency.

II. THEORY

A. THE NON-ABSORPTIVE CASE

A rectangular cavity of dimensions l_x, l_y, and l_z is excited by a sound source at $x = 0$. Let the cavity be acoustically terminated at $x = l_x$ in such a way that complete absorption of the incident acoustic energy takes place. That changes the cavity into a close approximation to an infinite waveguide. Let all other boundaries be pressure release.

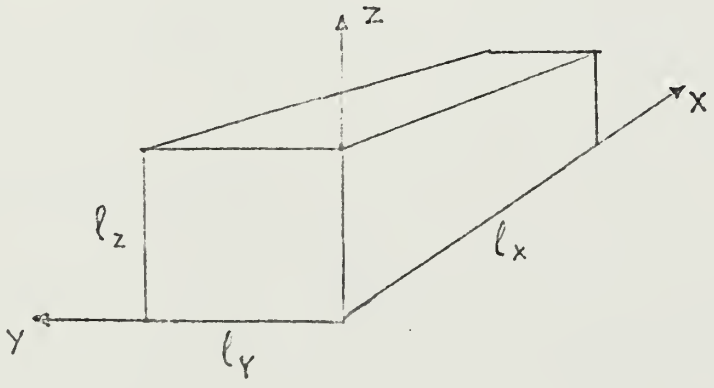

The theoretical cavity

FIGURE 1

A well-known solution of the wave equation for the velocity potential with these boundaries is

$$\Phi = \sin k_2 y \sin k_3 z \cos(\omega t - k_1 x) \tag{2.1}$$

For simplicity a unit amplitude is chosen. The k_i's must satisfy

$$k_2 = \frac{m\pi}{\ell_y} \quad , \quad k_3 = \frac{n\pi}{\ell_z} \quad , \quad \text{where } m, n = 1, 2, 3\ldots$$

and $\quad k_1 = (k^2 - k_2^2 - k_3^2)^{\frac{1}{2}}$, where $k = \omega/c$.

Let the upper boundary be perturbed by a standing surface wave of the form $\alpha \cos\gamma x \cos\Omega t$. If we define a perturbation constant $\epsilon = a/l_z$ and a function

$$F(x,t) = -l_z \cos\gamma x \cos\Omega t$$

we have boundaries at

$$z = 0$$

$$\text{and } z = l_z + \epsilon F(x,t) = l_z (1 - \epsilon \cos\gamma x \cos\Omega t) \quad (2.2)$$

on which $\Phi = 0$.

Assume there exists a solution

$$\Phi = \Phi_1 + \sum_{n=1}^{\infty} \epsilon^n \Phi_{n+1} \quad (2.3)$$

where Φ_1 , given by Eq. 2.1, is the solution without boundary fluctuations, and the remaining terms are contributions due to the fluctuating boundary.

A Taylor series expansion of Eq. 2.3 about l_z yields

$$\Phi = \Phi_1(l_z) + (z-l_z)\left.\frac{\partial \Phi_1}{\partial z}\right|_{l_z} + \frac{1}{2}(z-l_z)\left.\frac{\partial^2 \Phi_1}{\partial z^2}\right|_{l_z} + \cdots \quad (2.4)$$

$$+ \epsilon \Phi_2(l_z) + \epsilon (z-l_z)\left.\frac{\partial \Phi}{\partial z}\right|_{l_z} + \cdots$$

$$+ \epsilon^2 \Phi_3(l_z) + \cdots$$

Evaluating Eg. 2.4 at $z = l_z + \epsilon F(x,t)$ and collecting terms of equal power of ϵ leads to boundary conditions

$$\Phi_2\Big|_{l_z} = - F(x,t) \frac{\partial \Phi_1}{\partial z}\Big|_{l_z} \tag{2.5}$$

$$\Phi_3\Big|_{l_z} = - F(x,t) \frac{\partial \Phi_2}{\partial z}\Big|_{l_z} \tag{2.6}$$

etc.

Furthermore, since we have $\Phi\big|_{z=0} = 0$, then $\Phi_n\big|_{z=0} = 0$. The Φ_n's have to satisfy the wave equation separately since superposition applies. We require $\epsilon^n \Phi_{n+1} < \epsilon^{n-1} \Phi_n$. If we have $\epsilon \Phi_2 < \Phi_1$ and $\epsilon^2 \Phi_3 \ll \epsilon \Phi_2$, it is sufficient just to calculate Φ_2 . An investigation of Φ_3 is done in Appendix A.

From Eq. 2.1 and Eq. 2.5 we obtain

$$\Phi_2\Big|_{l_z} = k_3 l_z \sin k_2 y \cos(\omega t - k_1 x) \cos \gamma x \cos \Omega t \tag{2.7}$$

Eq. 2.7 can be decomposed into four traveling waves of frequencies $\omega \pm \Omega$ and wave numbers $k_1 \pm \gamma$. Each of these must be multiplied by some function of z such that each term satisfies the wave equation [9, 10]. This leads to the solution

$$\begin{aligned}\Phi_2 = G(\gamma) \Big[& \cos[(\omega+\Omega)t - (k_1+\gamma)x] \sin \mu_1 z / \sin \mu_1 l_z \\ & + \cos[(\omega+\Omega)t - (k_1-\gamma)x] \sin \mu_2 z / \sin \mu_2 l_z \\ & + \cos[(\omega-\Omega)t - (k_1+\gamma)x] \sin \mu_3 z / \sin \mu_3 l_z \\ & + \cos[(\omega-\Omega)t - (k_1-\gamma)x] \sin \mu_4 z / \sin \mu_4 l_z \Big]\end{aligned} \tag{2.8}$$

where $$G(y) = \frac{1}{4} \ell_z k_3 \sin k_2 y$$

and $$\mu_1^2 = \left(\frac{\omega+\Omega}{c}\right)^2 - (k_1+\gamma)^2 - k_2^2$$

$$\mu_2^2 = \left(\frac{\omega+\Omega}{c}\right)^2 - (k_1-\gamma)^2 - k_2^2$$

$$\mu_3^2 = \left(\frac{\omega-\Omega}{c}\right)^2 - (k_1+\gamma)^2 - k_2^2$$

$$\mu_4^2 = \left(\frac{\omega-\Omega}{c}\right)^2 - (k_1-\gamma)^2 - k_2^2 \quad .$$

Since $\omega \gg \Omega$, it is sufficient to approximate $\omega \doteq \omega \pm \Omega$ in the expressions for the μ_i's and we obtain

$$\mu_1 \doteq \mu_3 \doteq k_3 \left(1 - \frac{2k_1/\gamma + 1}{(k_3/\gamma)^2}\right)^{\frac{1}{2}} \qquad (2.9)$$

$$\mu_2 \doteq \mu_4 \doteq k_3 \left(1 - \frac{1 - 2k_1/\gamma}{(k_3/\gamma)^2}\right)^{\frac{1}{2}} \qquad (2.10)$$

With these approximations, and definition of

$$S_i = \frac{\sin \mu_i z}{\sin \mu_i \ell_z} \quad , \qquad i = 1,2 \quad .$$

the solution of Φ_2 simplifies to

$$\Phi_2 = G(y) C \cos \Omega t \cos[(\omega t - k_1 x) + \varphi] \qquad (2.11)$$

where $$C^2 = S_1^2 + S_2^2 + 2 S_1 S_2 \cos 2\gamma x$$

and $$\tan \varphi = \frac{S_1 - S_2}{S_1 + S_2} \tan \gamma x \quad .$$

Then the complete solution is

$$\Phi = \sin k_2 y \sin k_3 z \cos(\omega t - k_1 x) + \epsilon G(y) C \cos(\omega t - k_1 x + \varphi) \cos \Omega t \quad .$$

To simplify further one can measure the potential at an antinode of the surface wave and obtain

$$\Phi = \sin k_2 y \cos(\omega t - k_1 x)\left[\sin k_3 z + \frac{\epsilon k_3 \ell_z}{2}(S_1 + S_2)\cos \Omega t\right] \quad (2.12)$$

In the following discussion the acoustic wave will be restricted to the lowest propagating mode. Effects of higher modes will be discussed briefly in Appendix B.

The second term of Eq. 2.12 incorporates a fluctuation of the velocity potential with the frequency of the surface wave Ω, and an amplitude which is a function of the surface wave amplitude $\epsilon \ell_z$, the water depth ℓ_z, the receiver depth z, and a peculiar relation of the propagation constants contained in μ_1, and μ_2. If one holds the wave height $\epsilon \ell_z$ and frequency Ω of the surface wave constant, the interesting term of the solution is $S_1 + S_2$ which will be investigated as a function of k_1 (which itself is a function only of ω if k_2, k_3, and the speed of sound remain constant). To show the behavior of S_1 as a function of k_1/γ, let us rewrite μ_1, in the form $\mu_1 = k_3 h_1$

$$\text{where} \quad h_1 = \left(1 - \frac{2k_1/\gamma + 1}{(k_3/\gamma)^2}\right)^{\frac{1}{2}} , \quad (2.13)$$

Consider h_1 as a parameter which can be real or imaginary. If one plots k_3/γ versus k_1/γ for fixed values of h_1 a family of parabolas is generated according to the formula

$$\left(\frac{k_3}{\gamma}\right)^2 = \frac{2(k_1/\gamma) + 1}{1 - h_1^2} \quad .$$

Some of these parabolas are shown in Figure 2 as dotted lines. If h_1 is real (and since neither k_3/γ imaginary nor k_1/γ negative makes sense), we have $h_1 < 1$ for all $k_1/\gamma > 0$. This implies $\sin \mu_1 l_z < \sin k_3 l_z$, and hence s_1 is bounded. If h_1 is zero s_1 has the limit z/l_z. If h_1 is imaginary s_1 approaches zero as $|\mu_1|$ goes to infinity. The functional behavior of s_1 can be expressed as

$$S_1 = \begin{cases} \sin \mu_1 z / \sin \mu_1 l_z & , \quad 0 < h_1 < 1 \\ \sinh |\mu_1| z / \sinh |\mu_1| l_z & , \quad h_1 \text{ imaginary}, \; 0 < |h_1| < \infty. \end{cases}$$

s_1 and its derivative are continuous at $h_1 = 0$. Figure 3 shows sketches of s_1 at $z = l_z/2$ for three different k_3/γ. If one restricts the parameters k_1/γ and k_3/γ in such a way that they lie in the shaded area of Figure 2, s_2 becomes much larger than s_1 in the vicinity of resonance. <u>This restriction will be assumed for all further discussions and the experiment</u>.

The critical term in Eq. 2.12 is s_2. Let $\mu_2 = k_3 h_2$, then, like for s_1

$$\left(\frac{k_3}{\gamma}\right)^2 = \frac{2k_1/\gamma - 1}{h_2^2 - 1}$$

generates a family of parabolas with h_2 as parameter. For h_2 real

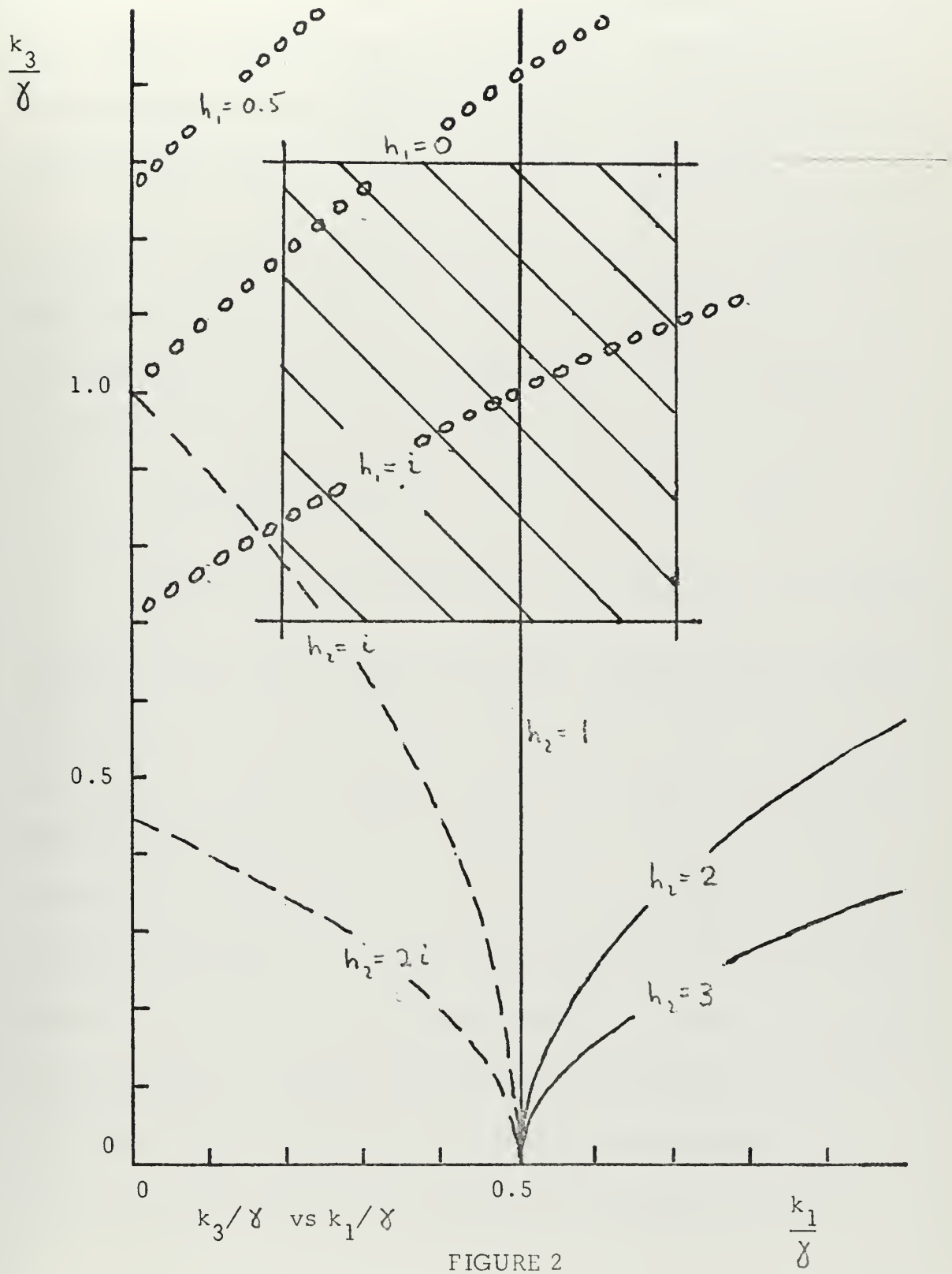
$\frac{k_3}{\gamma}$
$h_1 = 0.5$
$h_1 = 0$
$h_1 = i$
$h_2 = i$
$h_2 = 1$
$h_2 = 2$
$h_2 = 2i$
$h_2 = 3$
1.0
0.5
0
0
0.5
k_3/γ vs k_1/γ
$\frac{k_1}{\gamma}$

FIGURE 2

there exist an infinite number of h_2's such that $\sin k_3 h_2 l_z = \sin \mu_2 l_z = 0$ for $h_2 = 1,2,3\ldots$ which implies that s_2 has singularities for all integers h_2 provided the numerator does not equal zero. The lowest singularity or fundamental resonance occurs when $h_2=1$ or $2k_1 = \gamma$ and shows as a straight line in Figure 2. In general resonances occur when

$$\frac{k_1}{\gamma} = 0.5\left(h_2^2 - 1\right)\left(\frac{k_3}{\gamma}\right)^2 + 0.5 \quad , \quad h_2 = 1,2,3\ldots$$

Note that the fundamental resonance does not depend on k_3/γ while the higher ones do. For $h_2=0$, s_2 becomes z/l_z. For h_2 imaginary s_2 is a quotient of hyperbolic functions and is always less than one.

$$S_2 = \begin{cases} \sin\mu_2 z / \sin\mu_2 l_z & , \quad h > 0 \\ \sinh|\mu_2| z / \sinh|\mu_2| l_z & , \quad h \text{ imaginary} \ , \ 0 < |h_2| < \infty \end{cases}$$

s_2 and its derivative are continuous at $h_2=0$. Figure 4 shows sketches of s_2 at $z = l_z/2$ for two different k_3/γ. Figure 5 shows plots of $|s_1 + s_2|$ at $z = l_z$ as functions of k_1/γ for different values of k_3/γ. Since the obtained solution has an infinite number of resonances of unlimited amplitudes, the requirement $\epsilon_{n+1} < \epsilon_n$ is violated, and hence the solution is not valid in the vicinity of these resonances. However, the existence of resonances occurring at certain configurations of the propagation constants of acoustic and surface wave, receiver and channel depth can be deduced. A solution taking damping into account has to be sought for, to limit the amplitudes at resonance.

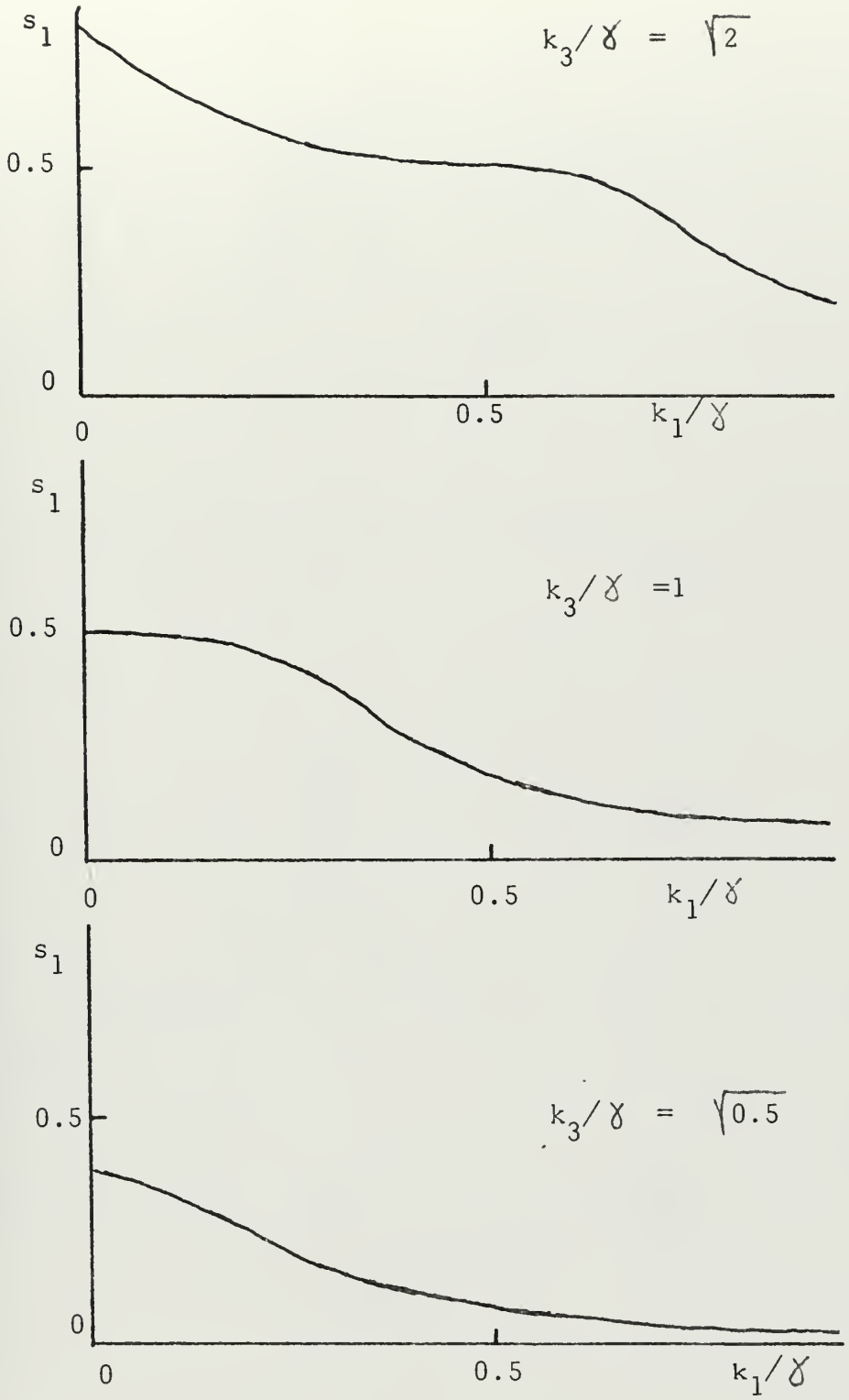

s_1 versus k_1/γ

FIGURE 3

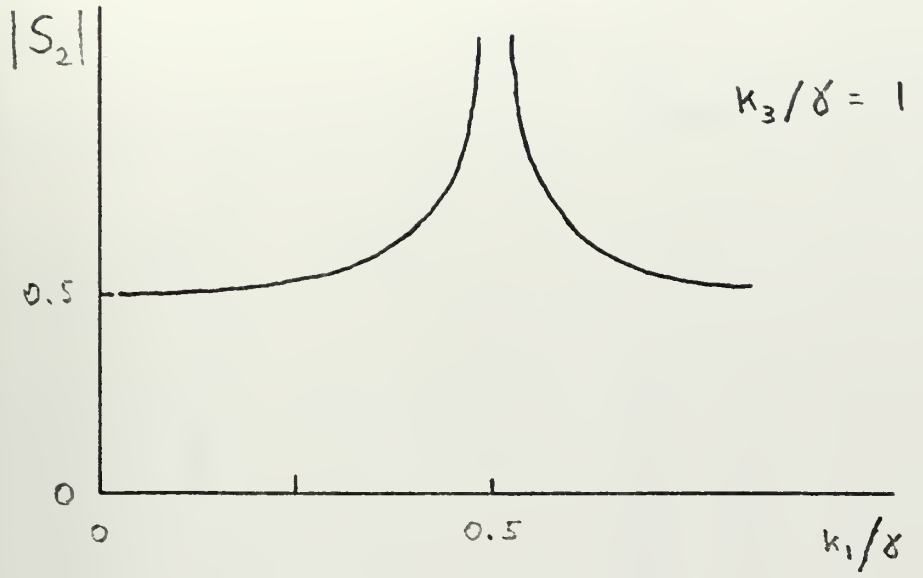

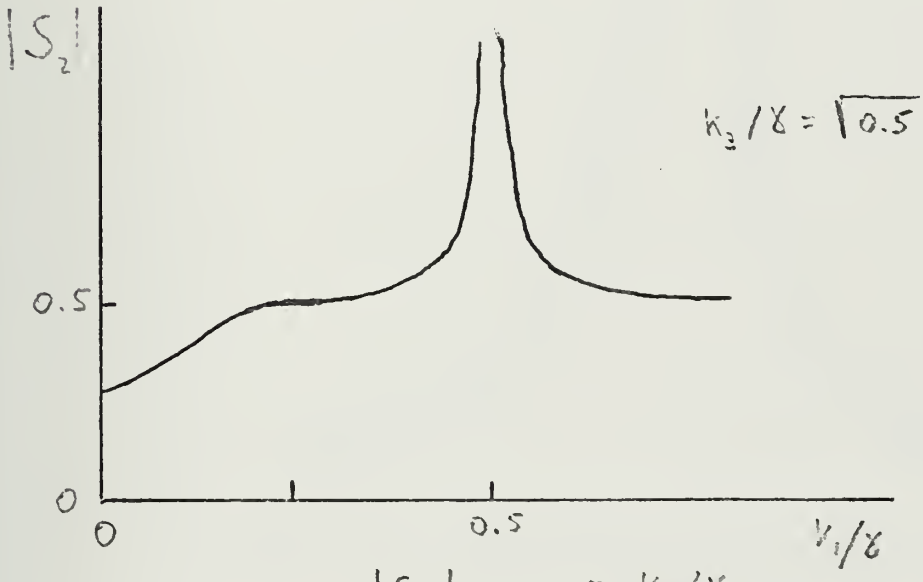

$|S_2|$ versus K_1/γ

FIGURE 4

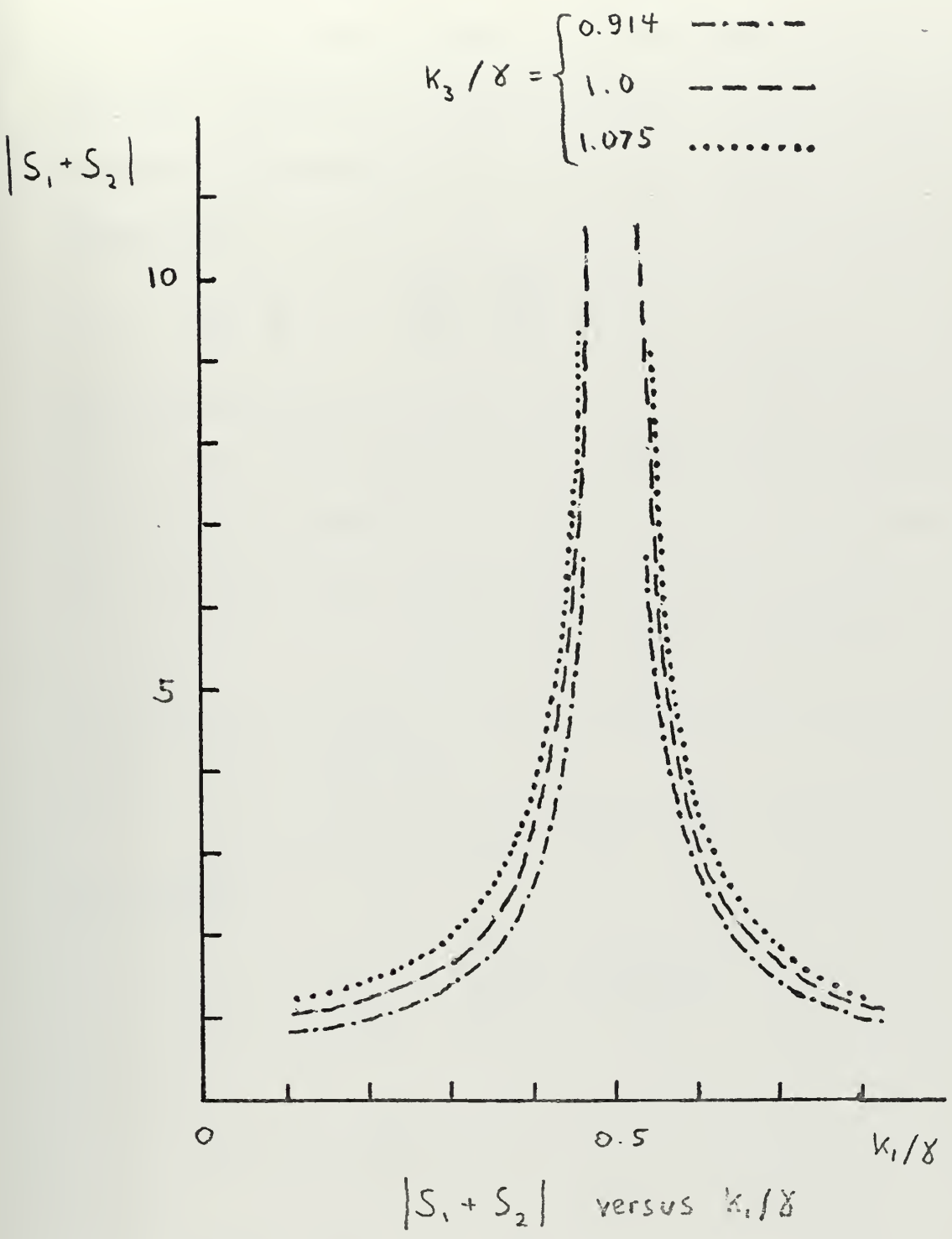

$|S_1 + S_2|$ versus K_1/γ

FIGURE 5

B. THE ABSORPTIVE CASE

To obtain a satisfactory solution in the vicinity of resonance, a lossy wave equation has to be found and solved. We will restrict this discussion to the fundamental resonance. We try an ad hoc differential equation [10]

$$\Box^2 \Phi - \frac{2\alpha}{c} \frac{\partial \Phi}{\partial t} = 0 . \tag{2.14}$$

The absorption coefficient must be obtained empirically for the experimental system since there will be loss mechanisms at the boundaries in addition to the usual viscous mechanism important in the fluid itself. Since the losses at the boundaries can be considered to lead to an attenuation of the signal as if they were distributed throughout the bulk of the fluid, assumption of Eq. 2.14 should not lead to any serious errors. It can be shown that

$$\cos(k_1 \pm \gamma)x \sin k_2 y \cos[(\omega \pm \Omega)t - \upsilon z] e^{-\beta z}$$

is a solution if

$$\upsilon^2 \doteq \frac{1}{2}\left[\mu^2 + \sqrt{\mu^4 + \left(\frac{2\alpha\omega}{c}\right)^2}\right] ,$$

$$\beta \doteq \alpha \frac{\omega}{c\upsilon} ,$$

$$\alpha/k \ll 1 ,$$

and $$\mu^2 \doteq \left(\frac{\omega}{c}\right)^2 - (k_1 \pm \gamma)^2 - k_2^2 .$$

Let us apply Eq. 2.14 to our system with the boundary conditions 2.2. We assume a solution of the form

$$\Phi_2 = A \sin k_2 y \sin(k_1 \pm \gamma)x \left[\sin\left((\omega \pm \Omega)t + \Theta + \upsilon z\right) e^{\beta z} - \sin\left((\omega \pm \Omega)t + \Theta - \upsilon z\right) e^{-\beta z} \right]$$

where A is some constant. With the help of Eq. 2.7 and proceed as in Part A, the solution of Eq. 2.14 can be written as

$$\Phi_2 = G(y) \cos \Omega t \left[R_1(z) \cos\left(\omega t - (k_1 + \gamma)x + \Theta_1(z)\right) + R_2(z) \cos\left(\omega t - (k_1 - \gamma)x + \Theta_2(z)\right) \right] \quad (2.15)$$

where $G(y) = 0.5\, l_2 k_3 \sin k_2 y$,

$$R_i^2(z) = \frac{\sin^2 \upsilon_i z \cosh^2 \beta_i z + \cos^2 \upsilon_i z \sinh^2 \beta_i z}{\sin^2 \upsilon_i l_z \cosh^2 \beta_i l_z + \cos^2 \upsilon_i l_z \sinh^2 \beta_i l_z}, \quad i = 1, 2$$

and $\Theta_i(z) = \tan^{-1}(\tan \upsilon_i l_z \coth \beta_i l_z) - \tan^{-1}(\tan \upsilon_i z \coth \beta_i z)$

The first expression of Eq. 2.15 in brackets can be neglected according to the restriction of the parameters k_1/γ and k_2/γ made in Part A. A typical ratio of R_2/R_1 was computed as 100 in the vicinity of resonance. Since $\beta_2 z$ and $\beta_2 l_z$ are both much less than one, $R_2(z)$ can be approximated as

$$R_2(z) \doteq \left(\frac{\sin^2 \upsilon_2 z + (\beta_2 z)^2 \cos^2 \upsilon_2 z}{\sin^2 \upsilon_2 l_z + (\beta_2 l_z)^2 \cos^2 \upsilon_2 l_z} \right)^{\frac{1}{2}}$$

which at resonance and for $z = l_z/2$ reduces to

$$R_2(l_z/2) \doteq \frac{1}{\beta_2 l_z} .$$

The total solution of the problem can be written as

$$\Phi = \sin k_2 y \sin k_3 z \cos(\omega t - k_1 x) \qquad (2.16)$$
$$+ \tfrac{1}{2}\epsilon l_z k_3 \sin k_2 y \, R_2(z) \cos\left(\omega t - k_1 x + \gamma x + \Theta_2(z)\right)$$

To simplify Eq. 2.16 let $y = l_y/2$ and $z = l_z/2$. Then Φ becomes

$$\Phi = \left(1 + C^2 + 2C\cos\Theta\right)^{\frac{1}{2}} \cos\left[(\omega t - k_1 x) + \delta\right] \qquad (2.17)$$

where $C = \tfrac{1}{2}\epsilon l_z k_3 \, R_2(l_z/2) \cos\Omega t$,

$\Theta = \Theta_2(l_z/2) + \gamma x$,

and $\delta = \tan^{-1} \dfrac{C\sin\Theta}{1 + C\cos\Theta}$.

Since we deal with just one acoustic frequency and a monochromatic surface wave the phase angle δ of the signal is not important. Eq. 2.17 is equivalent to a phasor diagram (Figure 6). The phasor is attached with its end to the tip of the phasor of the undisturbed signal of magnitude one. The magnitude of C , representing the amplitude $\epsilon\Phi_2$, oscillates between A and B at angular frequency Ω . The difference of $|\overline{OA}|$ and $|\overline{OB}|$ is the peak to peak amplitude of the fluctuation. The amplitude of C varies as a function of Θ_2 . The tip of C generates an "eight"-shaped curve. The orientation of this curve depends upon γx . The special cases $\gamma x = 0$ and $\gamma x = \frac{\pi}{2}$ correspond to surface wave antinode and node respectively. Note that when $\overline{AB}$ becomes perpendicular to the phasor of the unperturbed signal there is a sudden drop of the fluctuation amplitude. For the special case $\gamma x = 0$ this drop occurs at resonance. For $\gamma x = \frac{\pi}{2}$ there

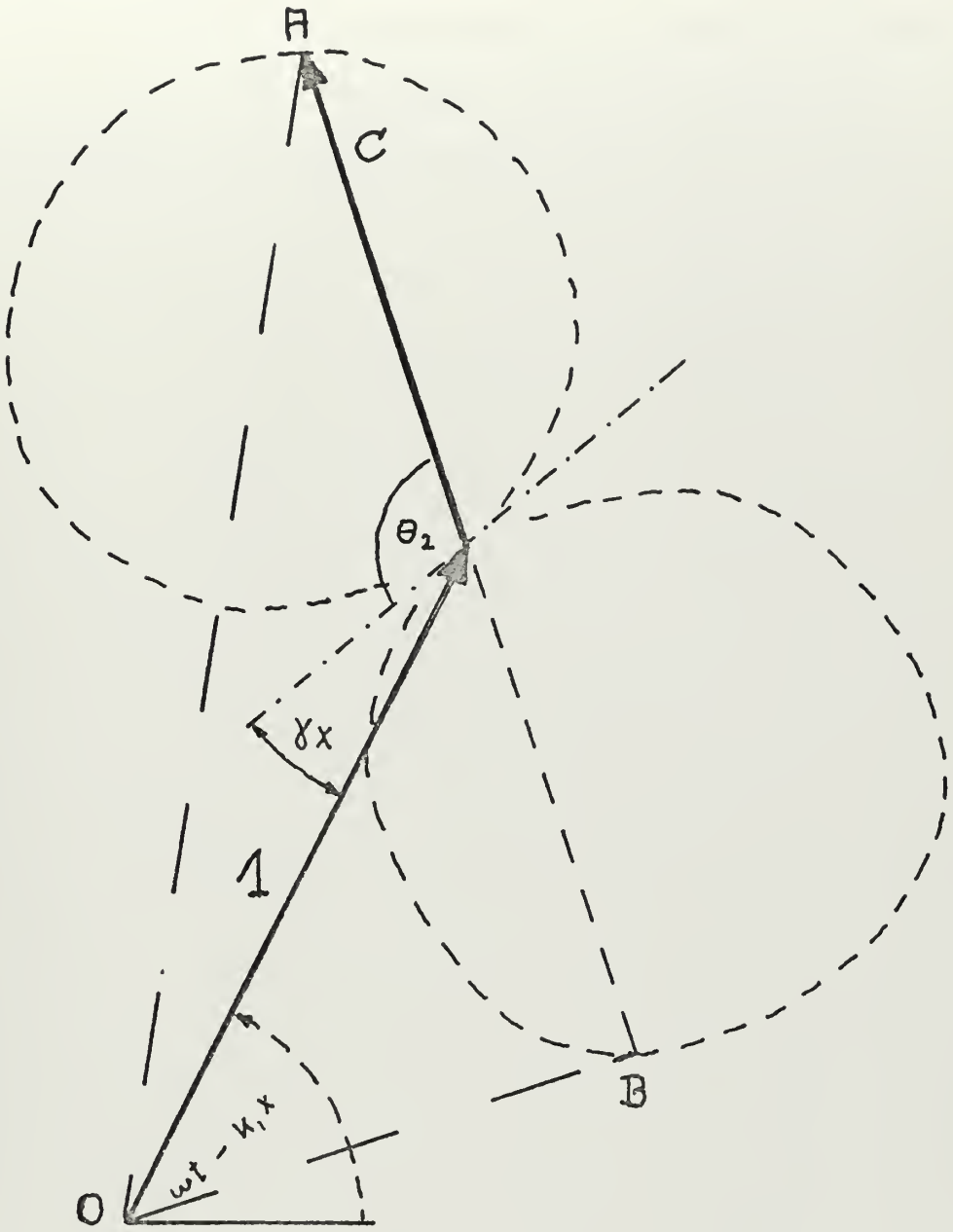

Phasor diagram of Eq. 2.17

FIGURE 6

is no such drop. It can be seen that the fluctuations are periodic and become more sinusoidal as C approaches the direction of the phasor of the unperturbed signal. Furthermore, under this condition the fluctuations become more linearly related to the wave height $\epsilon \ell_z$.

III. EXPERIMENT

A. DESCRIPTION

The object was to investigate the amplitude fluctuation of the signal as a function of k_1/δ . Special interest was to be given to the existence of the predicted resonances, their amplitudes, and the width of the resonance curves.

A 19.7 x 7 x 10 inch tank was chosen for the experiment. The walls consisted of 1 inch thick styrofoam which, against water, approximated pressure release boundaries. The tank was filled with water up to a height of 7 inches so that the water layer had a square cross section 7 inches on a side. The lowest propagating mode had a cut-off frequency of 5.89 kHz . The cut-off for the next higher mode was 7.2 kHz .

At one end of the tank a plane electrostatic source polarized with a 300V battery was used to excite the waveguide. The active face of the source was 3 inches square. At the other end of the waveguide absorbent rubber wedges were arranged to prevent reflection of the incident acoustic waves. The signal generator was operated in the tone-burst mode to generate a sequence of short acoustical pulses containing about sixteen cycles of the carrier frequency, and the wedges shifted until the returning echo was minimized. The standing wave ratio of the waveguide was reduced to about 1.1, representing a pressure

reflection coefficient at this end of the waveguide of about -0.09. At this same end a surface wave generator was installed. The generator consisted of a DC speed reducer motor controlled in rpm by an SCR power supply. The motor drove an adjustable cam which in turn drove a 4 x 6 inch paddle floating on the surface of the water. The paddle consisted of an upper layer of plywood glued on a layer of rubber foam to ensure pressure release conditions. A mechanical counter was connected to the cam to measure the frequency of the surface waves. To detect the wave amplitude, a thin stiff non-insulated wire was attached to a vertically movable sled which could slide on a vernier scale. The sled was connected electrically in series with a 1.5V battery, a microammeter, and the water (Figure 7). After the waveguide was excited by a standing surface wave pattern the wave height probe was shifted to an antinode and the wire carefully lowered down until the meter just started to deflect. The vernier scale reading was recorded. Then the wave generator was switched off, and the surface allowed to calm. Again the wire was lowered down until deflection of the meter just occurred. The scale was read, and the difference of the readings was the desired wave height.

The acoustic probe was a non-commercial one and had a cylinder of 1/8 inch diameter and 1/8 inch height as the active element (Figure 8). The probe was attached to a sled which was moveable in the x-direction. The active tip was positioned at the center of the

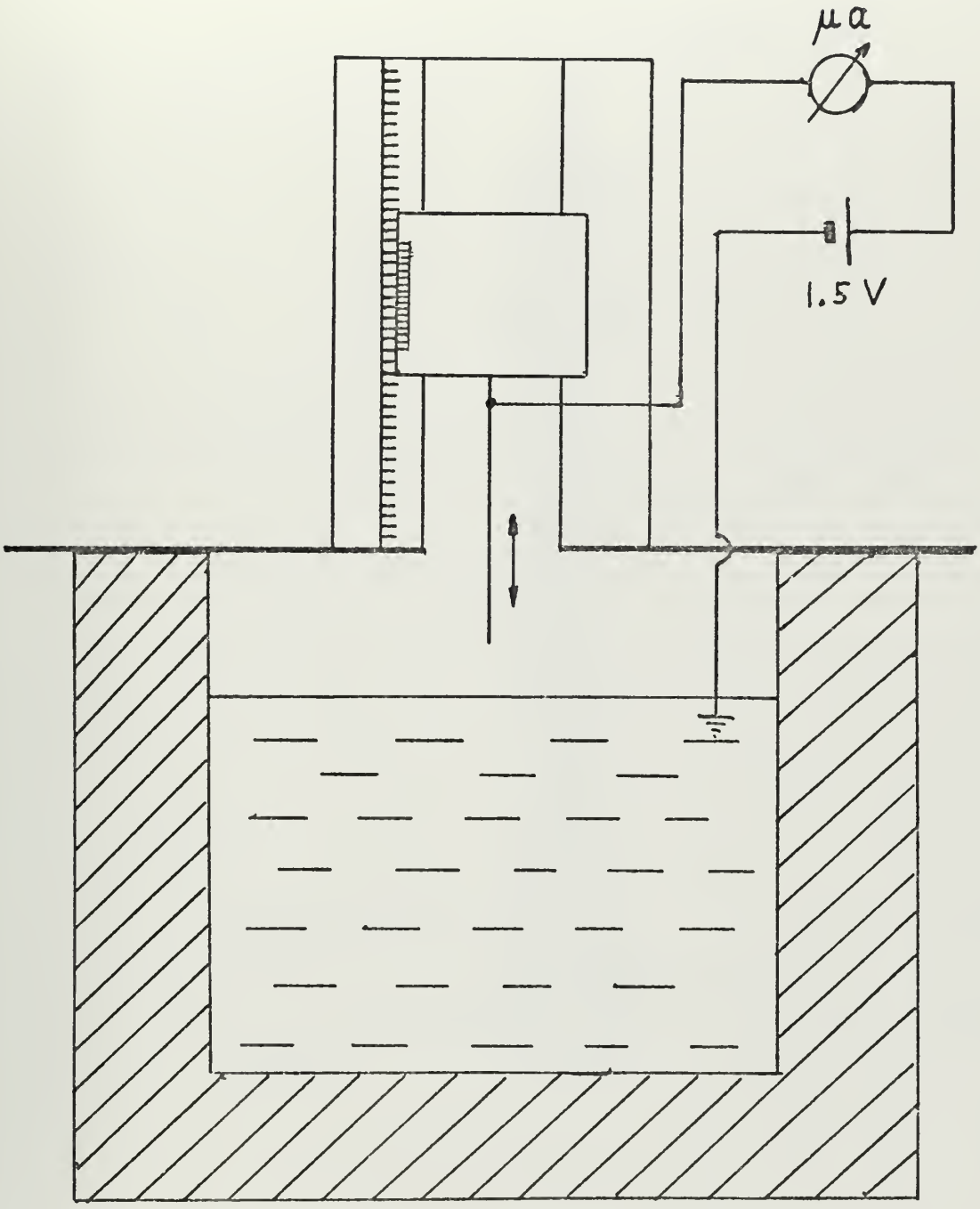

Sketch of the wave height probe

FIGURE 7

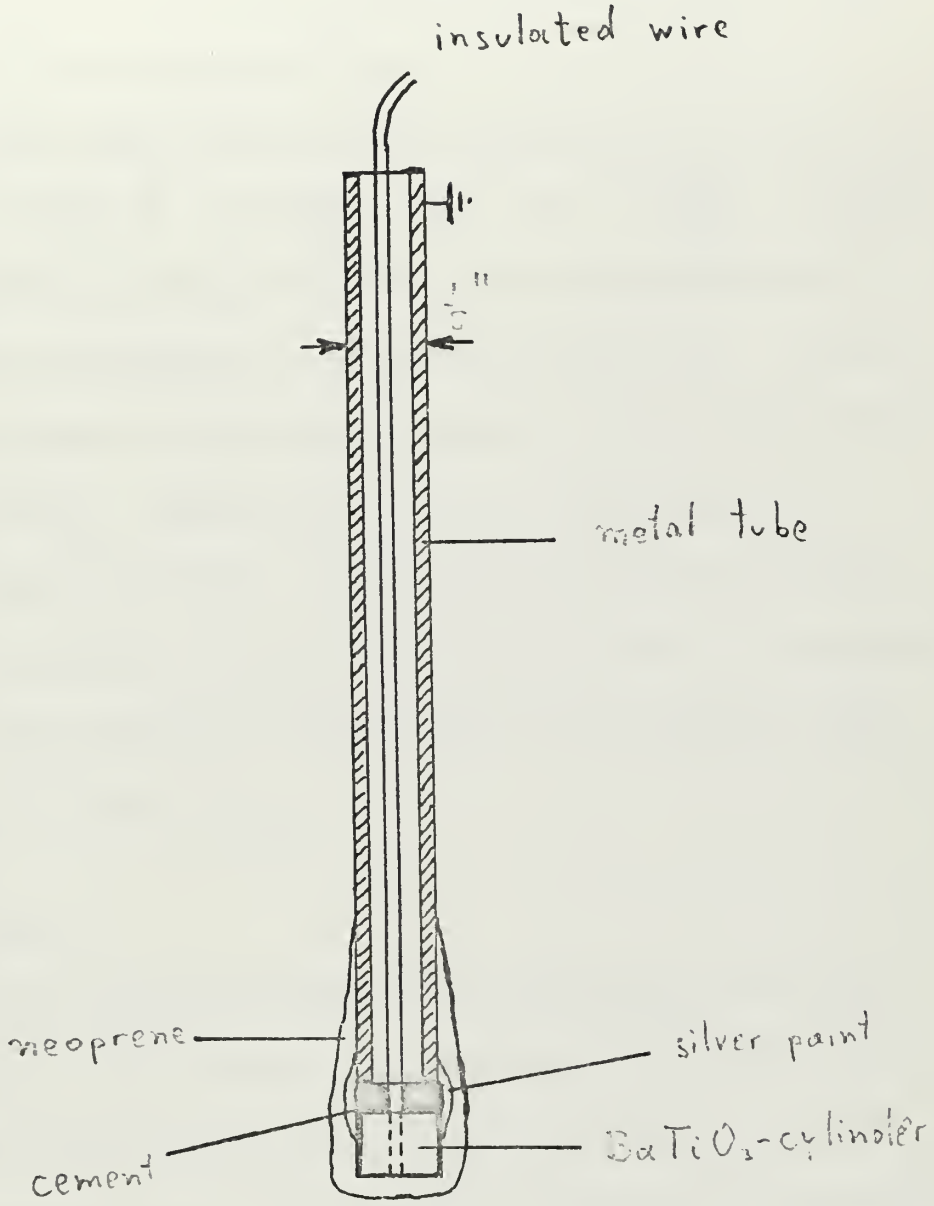

The acoustic probe

FIGURE 8

cross-section of the water layer. The detected signal was amplified 60 db, fed through a 1/10 - octave band filter, and displayed on a CRO. In some runs a wave analyser with bandwidth of 7 HZ was used instead of the 1/10 - octave band filter.

The acoustic probe will measure the acoustic pressure rather than the velocity potential ϕ . However, since $p = -\rho \frac{\partial \Phi}{\partial t} = -i\omega\rho \Phi$, the only distinction between p and Φ is a constant of proportionality $-i\omega\rho$ which corresponds to a phase shift in time of $\frac{\pi}{2}$ between pressure and potential. Since we are concerned with the relative phase between Φ_2 and Φ_1 , which will be the same as that between the associated pressure: p_2 and p_1 , we can ignore the distinction between pressure and potential in comparing experiment and theory. Alternatively, the relevant expressions for acoustic pressure can be obtained simply by operating on Φ with $-\rho \frac{\partial}{\partial t}$.

B. PROCEDURE

The experiment was restricted to an investigation of the fundamental resonance, since obtaining the conditions for the higher ones required either high frequencies which allowed more than one mode to propagate or surface waves longer than the available tank. A standing surface-wave pattern was generated and the frequency and wave height recorded. The wave length L was measured by taking the distance between three crests and averaging. Furthermore the wave length was estimated from the approximate formula $L = \frac{2\pi g}{\Omega^2}$ [11]. The observed

LIST OF EQUIPMENT

Signal generator	Hewlett Packard 200 CP
Gate	General Radio tone-burst generator 1396-17
Counter	Hewlett Packard 521 C
Amplifier	Tektronix 1121
1/10 - octave filter	General Radio 1564-A
Wave analyzer	Hewlett Packard 302A
CRO	Fairchild 766H
Motor	Bodine Electric NSE-11N
Speed control unit for motor	Seco Veri Volt 810

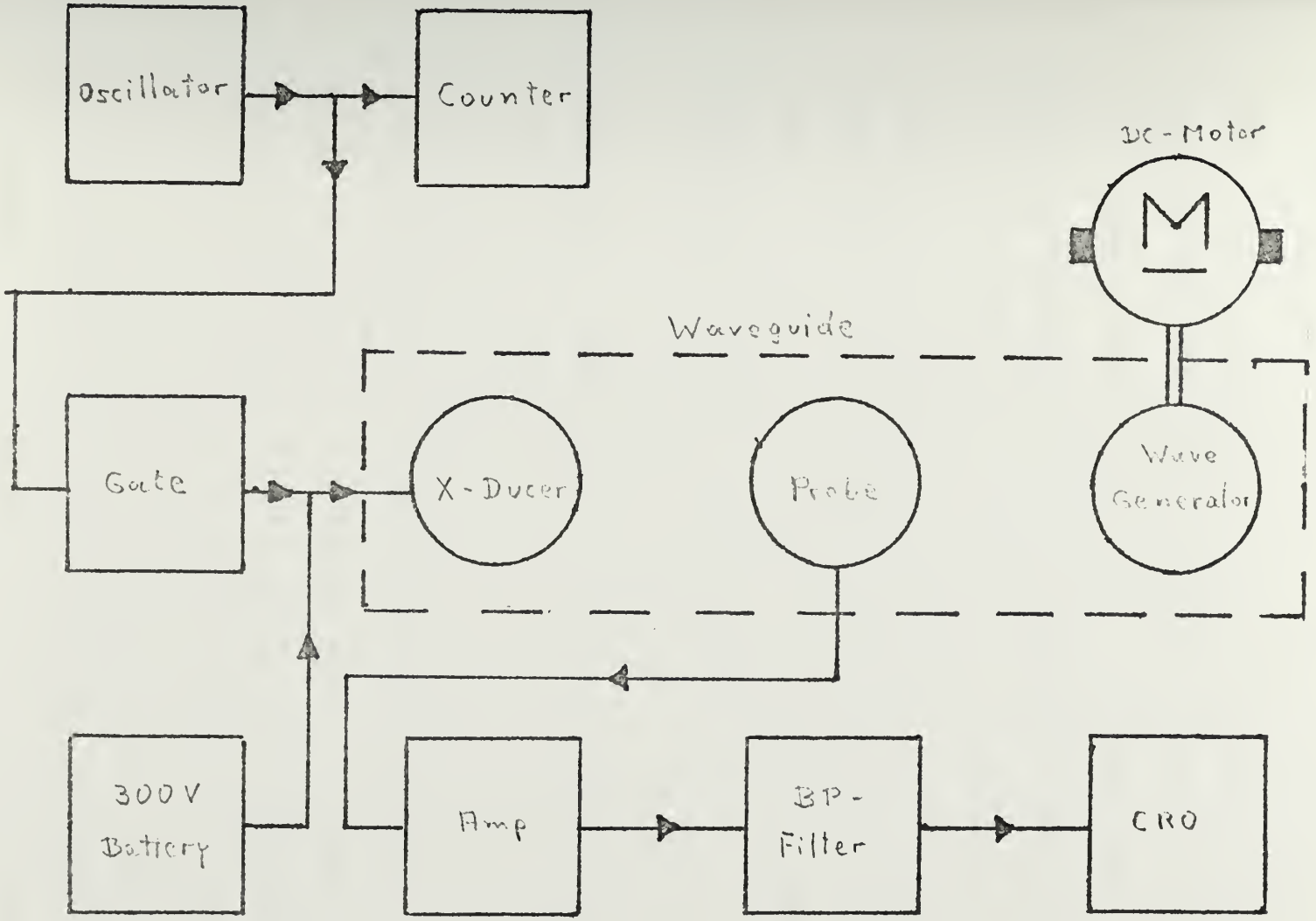

Block diagram of the system

FIGURE 9

and calculated wave length agreed to within ± 5%. They ranged from 25 to 45 cm. The sound source was driven at frequencies from 5.9 to 6.5 kHz in steps of 50 Hz. In the vicinity of the expected resonance the steps were decreased to 5 Hz. The probe was positioned beneath either a surface wave antinode or node. The amplitude fluctuations and the average amplitudes were read from the scope and recorded. The frequency and height of the surface waves were surveyed throughout the run. Measurement of λ_x was accomplished, after the surface had been allowed to calm, by the following method: The CRO was triggered by the driving voltage of the source. Then the probe was moved along the x-axis of the waveguide until the wave front on the scope had shifted one wave length. The distance the probe was moved was then the wave length in the x-direction (λ_x).

The effective absorption coefficient α of the system was obtained by removing the terminating rubber wedges and tuning the source to generate a standing acoustic wave. The removal of the terminating wedges allowed the standing wave to interact with the boundary at $x = \ell_x$. Since this boundary was much smaller than the others, the α determined for the cavity should be very similar to the actual attenuation coefficient for the traveling wave with the wedges in place. The frequency difference between the two half-power points was divided into the resonance frequency to calculate the Q of the closed cavity. This frequency was chosen close to the fluctuation resonance. The measured Q's were between 120 and 260 depending on whether the tank contained

fresh tap water or water which had been in the tank for several days during which the water could degas.

C. ERROR ANALYSIS

The amplitude of the fluctuation term of Eq. 2.16 at resonance and as observed at $z = \ell_z$ can be written as

$$A_{f,r} = \epsilon Q \left(\frac{k_3}{k}\right)^2 .$$

The error in calculating k_3/k can be neglected. The perturbation constant ϵ which is the ratio of wave height over waveguide depth depends on how exactly the wave height could be determined. The vernier scale of the wave height probe could be read to a precision of 0.05 mm. Several readings were taken at a calm water surface, as described in Section III. A, to check how well the data could be reproduced. The check resulted in a standard deviation of 0.12 mm. The applied wave amplitudes were on the average 1.1 mm. This yields an uncertainty in ϵ of about $\pm$ 10%. The quality factor Q could be obtained to an estimated accuracy of about $\pm$ 15%. Thus, the calculated value of $A_{f,r}$ has an uncertainty of $\pm$ 25%. The observed values of $A_{f,r}$ on the CRO bring in another uncertainty of $\pm$ 10% which gives a total possible uncertainty of about $\pm$ 35% between the calculated and measured amplitudes. Determination of the values of $k_1/2$ which correspond to the fluctuation amplitudes caused some problems. λ_x measured as indicated in III. B and calculated from the formulae $\lambda_x = 2\pi / k_1$ and $k_1^2 = k^2 - k_2^2 - k_3^2$ showed differences of 10%.

An explanation may be the fact that the width ℓ_y was not constant throughout the waveguide due to weak construction of the tank. Furthermore, the styrofoam walls may have absorbed some water which changed the assumed boundary conditions of pressure release. The measurements of λ_x and γ were accurate up to $\pm$ 5% each. The surface wave frequency Ω was sufficiently constant. Maximum changes of 1.5% were recorded. The wave height changed $\pm$ 0.1 mm. during one run. However, to obtain the theoretical curves of the fluctuations using a computer program, the wave height was averaged and assumed constant. Figure 10 shows a plot of fluctuation amplitude versus wave height at a frequency away from resonance. The fairly good linearity of the data makes the measurements of the amplitude fluctuation on the CRO and of the wave height trustworthy.

IV. RESULTS AND CONCLUSIONS

The results delivered by the theory are

a. There exist an infinite number of resonance conditions for the modulation of the acoustic signal. A major or fundamental resonance occurs when the surface wave length is one-half of the acoustic wave length in the x-direction. The damping coefficient of these resonances may tend to increase with frequency. If the pressure is measured close to a surface wave antinode there is a sharp dip in the fluctuation amplitude close to resonance.

b. The acoustic signal fluctuates at the frequency of the surface waves unless the phasor C in Figure 6 is perpendicular to the phasor of the undisturbed signal. In this case the acoustic fluctuations become small and occur at twice the frequency of the surface waves.

c. If the surface wave height is increased harmonics of the surface wave frequency will occur.

d. If the phase angle Θ of Eq. 2.17 is in the vicinity of 180 degrees, the signal fluctuates approximately sinusoidal and the fluctuation amplitude increases almost linearly with wave height of the surface wave until higher harmonics, as mentioned in c show up.

Several data were taken to verify these statements. Figure 10 shows a plot of fluctuation amplitude, denoted by $\Delta A/A$, versus wave height. This set of data was measured off resonance, i.e., Θ

was about 175°, and presents fairly good linearity. Figures 11, 12, 13 and 14 reveal the presence of the fundamental resonance at $k_1/\gamma = 0.5$. Figures 11, 12 and 13 which show plots of the fluctuation amplitude at a surface wave antinode indicate clearly the predicted dipping of the resonance curve at $k_1/\gamma = 0.5$. This dipping does not occur in Figure 14 since the probe was positioned at a surface wave node --i.e., Θ was equal to π at resonance. The dashed lines represent the theoretical resonance curves obtained from a computer program written to calculate the amplitude of Eq. 2.17.

In Figure 13 where the theoretical curves for antinode and node position of the probe are drawn one peak is much higher than the other one. An explanation may be that the probe was positioned slightly off an antinode. To show the occurrence of harmonics introduced by higher perturbation orders if the wave height is increased, two photographs (Figures 15a and 15b) of the modulation were taken for two different wave heights. The probe was placed at a surface wave antinode, and the acoustic signal was tuned to one of the resonance peaks. Figure 15a was obtained at a wave amplitude of 5.6 mm. corresponding to an ϵ of 0.03. The superposition of the first and second harmonics can easily be seen. Higher harmonics which might have been present were filtered out since a narrow band-pass filter was used. (The bandwidth was 7 HZ, and the center frequency was ω. The surface wave frequency was about 1.8 HZ. Thus the third harmonic had frequency components

$\omega \pm 5.4$ HZ which were beyond the edges of the passband.) The band-pass filter had to be used occasionally due to the presence of broad-band noise. For Figure 15b the wave amplitude was reduced to 1.4 mm. or $\epsilon = 0.008$. The modulation is almost monochromatic (Θ was about 135°).

The obtained data are semi-quantitatively consistent with the theory. The presence of the fundamental resonance at $k_1/\gamma = 0.5$, the dip of the resonance curve if $\Phi = \frac{\pi}{2}$, the appearance of the second harmonic, and the almost linear relationship between fluctuation amplitude and surface wave height can easily be seen. The wider and lower resonance curves obtained experimentally cannot be explained. Probable causes are:

1. The applied wave height might have been too large which violated the requirements for this perturbation theory to be sufficiently precise. $\epsilon \bar{\Phi}_2$ was of the order of 0.2 $\bar{\Phi}_1$. The use of smaller wave heights, however, caused problems in observing the fluctuations and measuring the wave amplitudes.

2. The unperturbed acoustic signal and surface wave were taken to be undamped.

3. The surface waves did not establish perfect standing wave patterns. (The nodes of the standing wave oscillated about 2 cm in the x-direction.)

No attempt was made, to obtain plots for higher resonances, since increasing the frequency allowed higher modes to propagate. The fluctuation terms of the different modes cannot simply be added because complicated phase terms come into being. The existence of these higher resonances was observed qualitatively.

The theory of the present paper explains the broadening effect of the modulation spectrum as it was observed by Scrimger [1] and D'Antonio [2]. An increase in ξ requires taking more terms of Eq. 2.3 into account which introduces harmonics of the modulation frequency as pointed out in Appendix A. If one were to apply this theory to shallow water in the ocean the statistics of the sea surface would have to be tied into the boundary conditions. The reflection coefficient of the ocean bottom, changes in water depth and sound velocity gradient would complicate the problem tremendously. However, one can suspect that the surface wave spectrum will resemble in shape plots of fluctuation amplitude versus acoustic frequency.

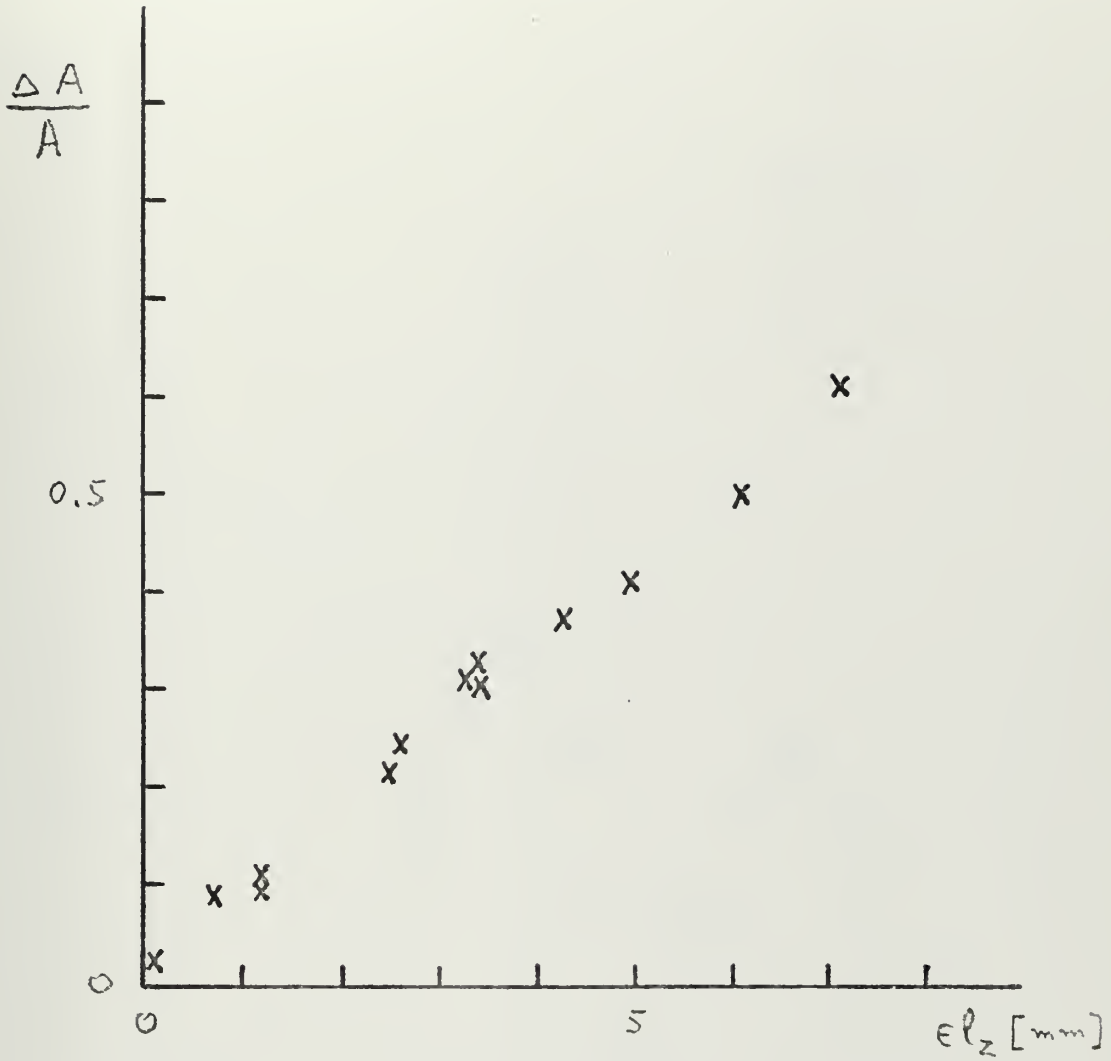

Acoustic amplitude fluctuation versus wave height

FIGURE 10

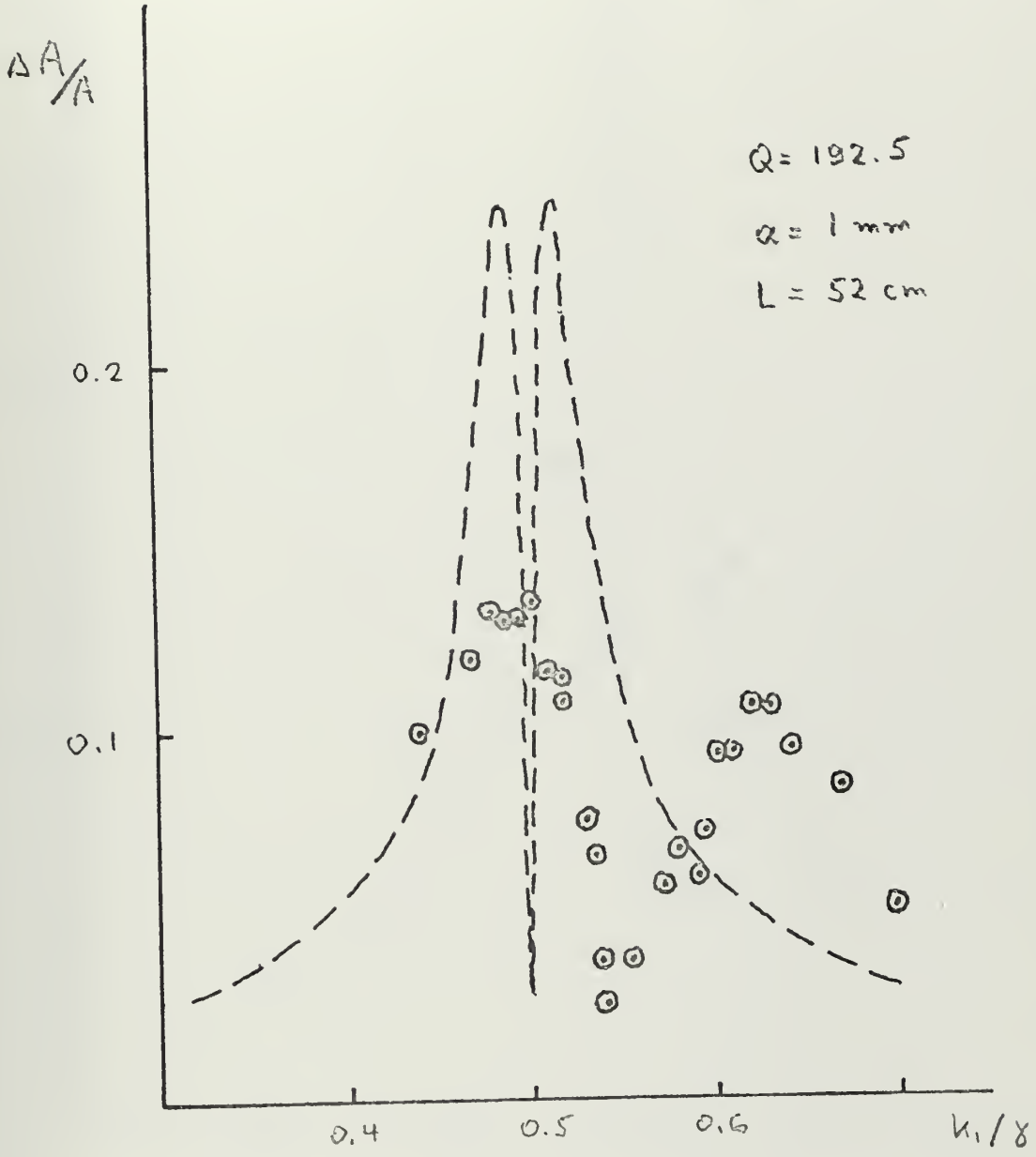

Acoustic amplitude fluctuation versus k_1/γ at an antinode

FIGURE 11

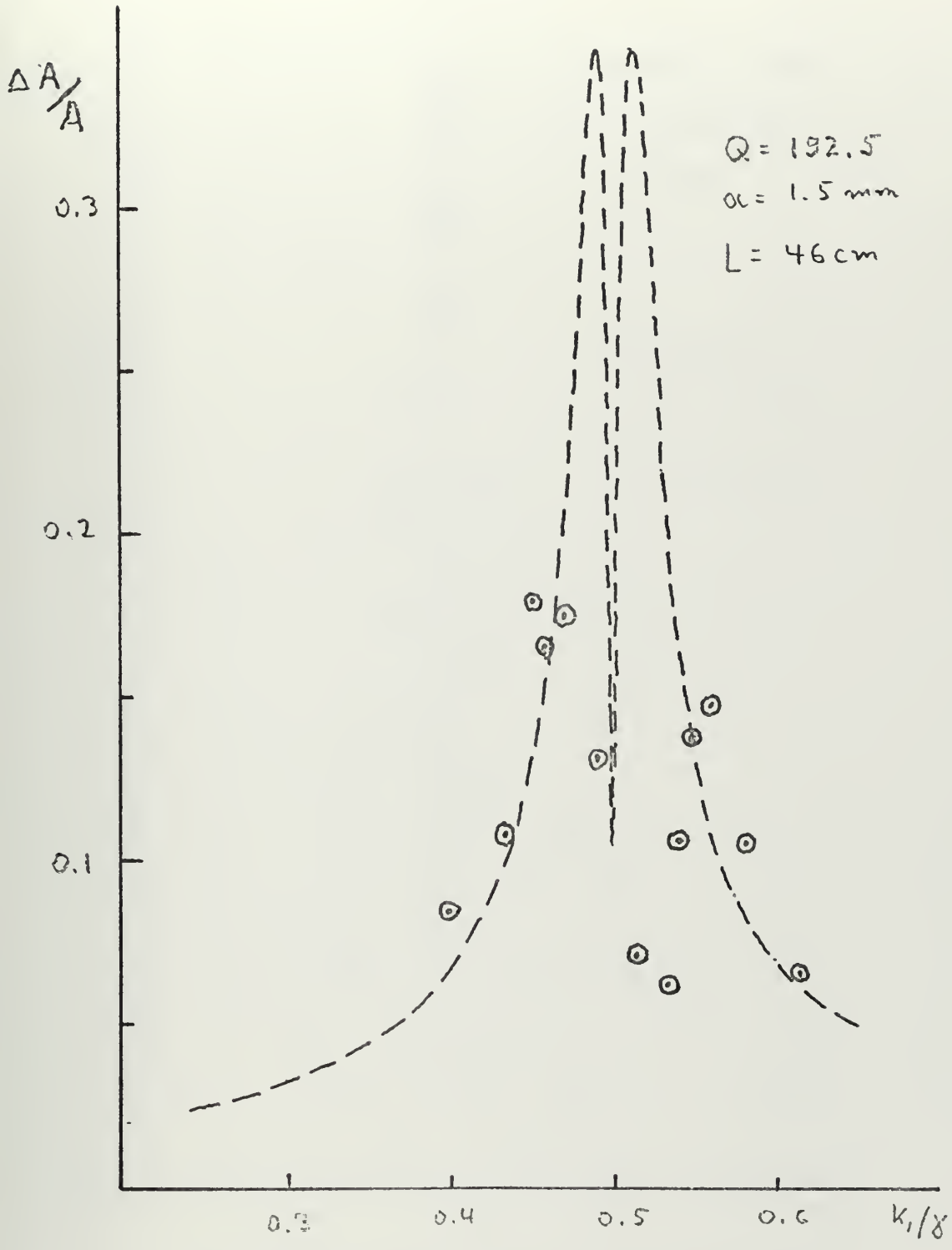

Acoustic amplitude fluctuation versus k_1/γ at an antinode

FIGURE 12

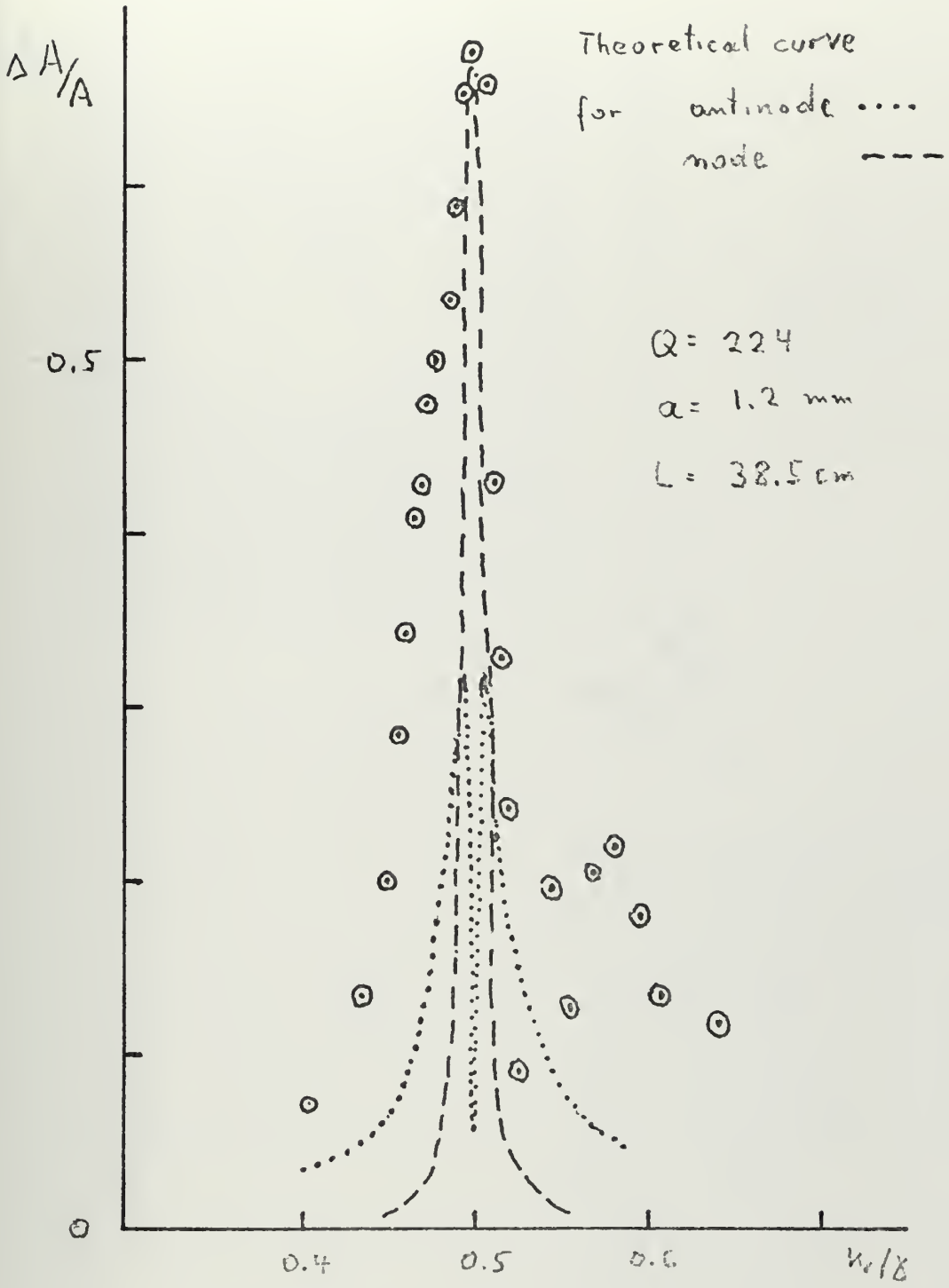

Acoustic amplitude fluctuation at an entinode

FIGURE 13

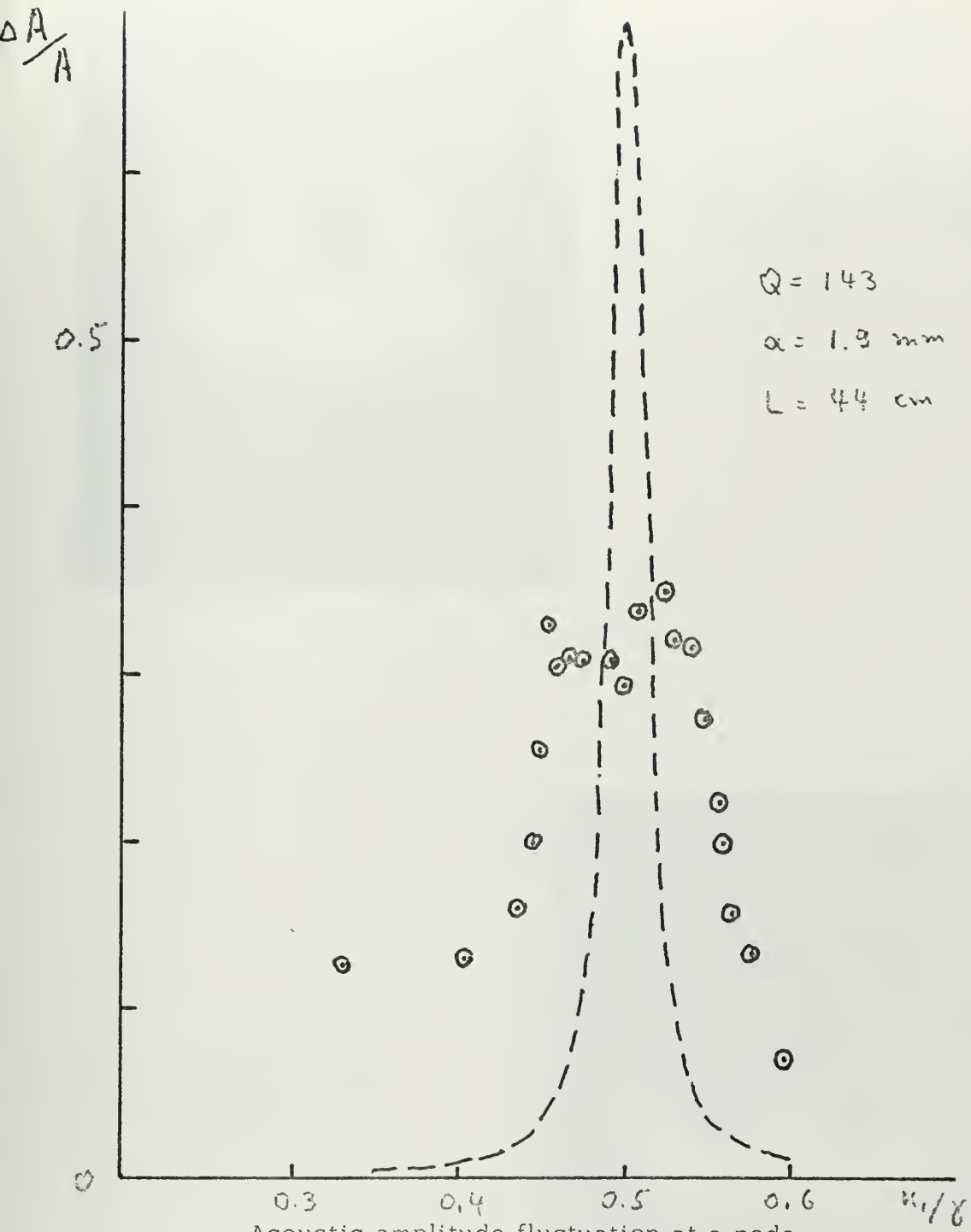

Acoustic amplitude fluctuation at a node

FIGURE 14

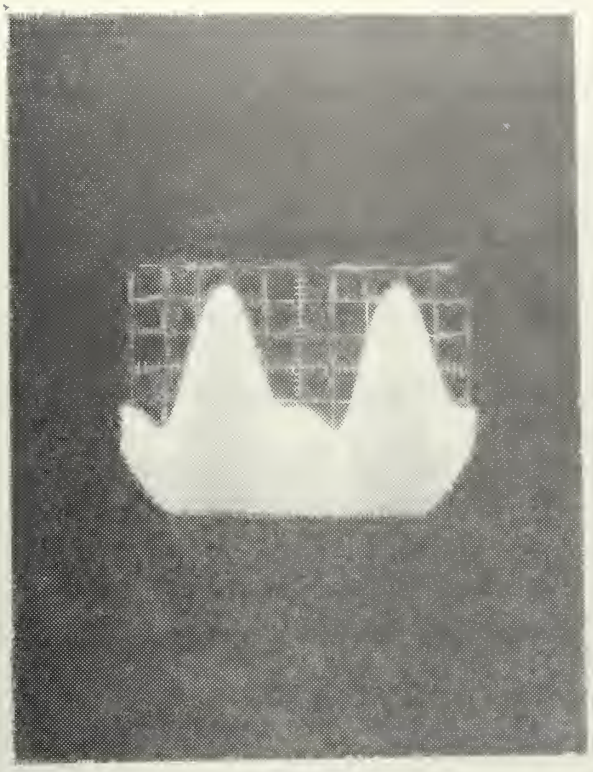

Fluctuations of amplitude
for $\varepsilon = 0.03$

FIGURE 15a

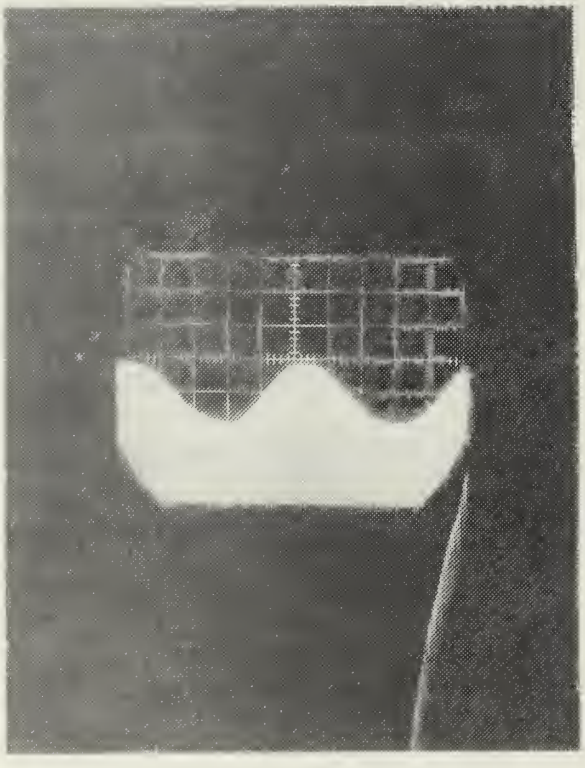

Fluctuations of amplitude
for $\varepsilon = 0.05$

FIGURE 15b

APPENDIX A

A BRIEF DISCUSSION OF Φ_3.

If one drops the restriction $\epsilon^2 \Phi_3 \ll \epsilon \Phi_2$ but keeps $\epsilon^2 \Phi_3 < \epsilon \Phi_2$ and $\epsilon^3 \Phi_4 \ll \epsilon^2 \Phi_3$ one has to consider Φ_3. $\Phi_3|_{\ell_2}$ can be obtained using Eq. 2.3, and Eq. 2.6 and neglecting S_1 since $S_2 \gg S_1$ close to resonance.

$$\begin{aligned}\Phi_3 = C \Big[& \cos[\omega t - (k_1+\gamma)x] \\ & + \cos[\omega t - (k_1-\gamma)x] \\ & + \cos[(\omega+2\Omega)t - (k_1+\gamma)x] \\ & + \cos[(\omega-2\Omega)t - (k_1+\gamma)x] \\ & + \cos[(\omega+2\Omega)t - (k_1-\gamma)x] \\ & + \cos[(\omega-2\Omega)t - (k_1-\gamma)x]\end{aligned}$$

where $C = \frac{1}{16} \epsilon k_3 \ell_2^2 \mu_2 \coth(\mu_2 \ell_2)$

Taking $\Phi_3|_{\ell_2}$ at an antinode of the surface wave one obtains

$$\Phi_3|_{\ell_2} = 2C \cos(\omega t - k_1 x)[1 + 2\cos 2\Omega t].$$

Without solving for Φ_3 the following facts can be noticed. The fluctuation now occurs at twice the surface wave frequency. If one increases the wave height, one has to consider Φ_4, Φ_5 etc. which bring up all the harmonics of Ω.

APPENDIX B

HIGHER MODES

Allowing higher modes than the lowest one to propagate introduces more resonances. Let the eigen values k_{3n} be defined by $n\pi / l_z$. Then there exist resonances for S_1 if $h_1 = m/n$, where m and n are integers and $m < n$. For S_2 we have an infinite number of resonances if $h_2 = m/n$, where m and n are integers. Taking all higher modes into account the potential can be written as

$$\Phi = \sum_{n=1}^{\infty} A_n \left(\overset{1}{\Phi}_{1n} + \epsilon \overset{1}{\Phi}_{2n} \right)$$

where $\overset{1}{\Phi}_{1n} = \cdots k_{2n} y \cdots k_{3n} z \cos(\omega t - k_1 x)$

and $\overset{1}{\Phi}_{2n} = G(y)_n C_n \cos \pi t \cdot \cos[(\omega t - k_1 x) + \varphi_n]$

$G(y)_n$ and C_n can be obtained by setting $k_3 = k_{3n}$ and $k_2 = k_{2n}$ in $G(y)$ and C of Eq. 2.11. The coefficients A_n can be determined from the source configuration and the boundaries using Fourier analysis. If the water surface is disturbed by surface waves of more than one frequency, the fluctuation terms $\overset{1}{\Phi}_{1n}$ having different phase angles φ_n have to be added statistically.

APPENDIX C

CALCULATION OF

Let a cavity of dimensions ℓ_x, ℓ_y, ℓ_z have a potential of $\Phi = \Phi_0 e^{i\omega t}$ at $z=0$ and zero at $z=\ell_z$. Assume a solution of Eq. 2.14 of the form

$$\Phi = \sin k_2 y \sin k_1 x \left(A e^{i(\omega t - k_3 z) - \eta z} + B e^{i(\omega t + k_3 z) \eta z} \right)$$

Substituting this solution into Eq. 2.14 yields

$$\eta = \alpha \frac{\omega}{c k_3}$$

From the boundary conditions one obtains

$$A = -B$$

and $$|A| = \frac{\Phi_0}{2} \frac{1}{\left((\eta \ell_z)^2 \cos^2 k_3 \ell_z + \sin^2 k_3 \ell_z \right)^{\frac{1}{2}}}$$

where $\eta \ell_z$ is assumed to be much smaller than one. k_3 can be expanded as

$$k_3 \doteq k_{3r} + \frac{\omega_r \Delta\omega}{c^2 k_{3r}} = k_{3r} + \Delta k_3$$

where k_{3r} is k_3 at resonance, ω_r the resonance radian frequency and $\Delta\omega$ the deviation of radian frequency from resonance. For resonance let $\sin k_{3r} \ell_z = 0$, $\cos k_{3r} \ell_z = 1$, and let $\Delta\omega$ be denoted by $\Delta\omega_0$. Then Q is given by $\omega_r / 2\Delta\omega_0$. The amplitude at resonance can be approximated by

$$|A|_r \doteq \frac{\Phi_0}{2} \frac{1}{\eta \ell_z}$$

and the amplitude at the one-half power points as

$$|A|_{0.707} = \frac{1}{2} \Phi_0 / \left[\eta^2 \ell_z^2 + \Delta k_3^2 \ell_z^2 \right]^{\frac{1}{2}}$$

Since $|A|_r / |A|_{0.707} = \sqrt{2}$

$$\eta = \frac{1}{2} k^2 \frac{1}{K_3 Q} \quad \text{and} \quad \alpha = \frac{1}{2} \frac{k}{Q} .$$

Hence

$$\eta = \beta .$$

BIBLIOGRAPHY

1. Scrimger, J. A., Signal Amplitude and Phase Fluctuations induced by Surface Waves in Ducted Sound Propagation, J. Acoust. Soc. Am., Vol. 33, February, 1961: 239-247.

2. D'Antonio, R.A. and Hill, R.F., Distortion of Underwater Acoustic Signals Reflected from a Time and Space Random Surface, J. Acoust. Soc. Am., Vol. 38, November,1965: 701-706.

3. Wood, A.B., Model Experiments and Sound Propagation in Shallow Seas, J. Acoust. Soc. Am., Vol. 31, September, 1959: 1213-1234.

4. Urick, R.J., Lund, G.R., and Bradley, D.L., Observations of Fluctuation of Transmitted Sound in Shallow Water, J. Acoust. Soc. Am., Vol. 45, March 1969: 683-690.

5. Clay, C. S., Effect of a Slightly Irregular Boundary on the Coherence of Waveguide Propagation, J. Acoust. Soc. Am., Vol. 36, May 1969: 833-837.

6. Clark, J.G. and Weinberg, N.L., Refracted, Bottom-Reflected Ray Propagation in a Shallow Water Channel with Slowly Time-Varying Stratification, J. Acoust. Soc. Am., Vol. 48, July, 1970: 92(A).

7. Westervelt, P.J., Halpin, H., and Williams, A.O., Wave-Induced Fluctuations in Shallow-Water Sound Propagation, J. Acoust. Soc. Am., Vol. 41, June, 1967: 1617(A).

8. Tanakanov, O.S., Sound Fluctuations During Propagation in a Shallow Layer of Water, Soviet Physics, Vol. 7, October-December, 1961: 185-189.

9. Jordan, W.E., Jr., Preliminary Investigation of the Effect of Surface Fluctuations on Sound Amplitude in Guided Mode Propagation, Master Thesis, 1970, Naval Postgraduate School.

10. Coppens, A. B., Private communication.

11. Bascom, Willard, Waves and Beaches

INITIAL DISTRIBUTION LIST

		No. Copies
1.	Defense Documentation Center Cameron Station Alexandria, Virginia 22314	2
2.	Library, Code 0212 Naval Postgraduate School Monterey, California 93940	2
3.	Assoc Professor A. B. Coppens, Code 61Cz Department of Physics Naval Postgraduate School Monterey, California 93940	2
4.	FGN, DOKZENT BW-SEE 53 Bonn Fr. Ebert Allee 34 W-Germany	1
5.	Marineamt, FGN U/UO AusbM 294 Wilhelmshaven W-Germany	1
6.	KPTLT Rolf Ebert 294 Wilhelmshaven Marineamt - 1NMWa W-Germany	1

DOCUMENT CONTROL DATA - R & D

(Security classification of title, body of abstract and indexing annotation must be entered when the overall report is classified)

1. ORIGINATING ACTIVITY (Corporate author)	2a. REPORT SECURITY CLASSIFICATION
Naval Postgraduate School Monterey, California 93940	Unclassified
	2b. GROUP

3. REPORT TITLE

A Study of the Influence of Gravity Waves in a Water-filled Waveguide

4. DESCRIPTIVE NOTES (Type of report and inclusive dates)

Master's Thesis; December 1971

5. AUTHOR(S) (First name, middle initial, last name)

Rolf H. Ebert

6. REPORT DATE	7a. TOTAL NO. OF PAGES	7b. NO. OF REFS
December 1971	52	11

8a. CONTRACT OR GRANT NO.	9a. ORIGINATOR'S REPORT NUMBER(S)
b. PROJECT NO.	
c.	9b. OTHER REPORT NO(S) (Any other numbers that may be assigned this report)
d.	

10. DISTRIBUTION STATEMENT

Approved for public release; distribution unlimited

11. SUPPLEMENTARY NOTES	12. SPONSORING MILITARY ACTIVITY
	Naval Postgraduate School Monterey, California 93940

13. ABSTRACT

A simple theory is developed which describes the fluctuation of a sound signal due to the influence of a standing gravity wave in a water-filled waveguide with idealized boundary conditions. The theory predicts a strong resonance of the fluctuation if the wave length of the surface wave is one-half of the acoustic wave length. The presence of this resonance is verified experimentally.

KEY WORDS	LINK A		LINK B		LINK C	
	ROLE	WT	ROLE	WT	ROLE	WT
Waveguide						
Perturbation						
Sound Propagation						
Normal Modes						